THE ASTROPHYSICAL JOURNAL, 262:253–262, 1982 November 1


# INFRARED PHOTOMETRY OF THE X-RAY BINARY 2A 1822–371: A MODEL FOR THE ULTRAVIOLET, OPTICAL, AND INFRARED LIGHT CURVE

KEITH O. MASON[1,2]
Mullard Space Science Laboratory, University College London
AND
FRANCE A. CÓRDOVA[1]
Earth and Space Sciences Division, Los Alamos National Laboratory
*Received 1982 January 21; accepted 1982 April 13*

## ABSTRACT

The light curve of the 5.57 hr binary X-ray source 2A 1822–371 has been measured at 1.25 $\mu$m. It is found to be similar in shape and depth of modulation to the optical light curve. Thus the marked variation in the shape of the light curve with wavelength, which was found previously in the ultraviolet region, does not persist at longer wavelengths. Measurements at 1.25 $\mu$m, 1.65 $\mu$m, and 2.2 $\mu$m show that the spectrum of the star in the near-infrared is consistent with the $\lambda^{-4}$ Rayleigh-Jeans tail of the optical spectrum. The entire spectrum at maximum light from 0.11 $\mu$m to 2.2 $\mu$m can be approximated well by a blackbody model with a temperature of $2.7 \times 10^4$ K reddened by an amount corresponding to $E(B-V) = 0.2$.

A model for the ultraviolet, optical, and infrared light curves is constructed, based on the azimuthal structure in the thickness of the outer accretion disk that was deduced previously from fits to the X-ray light curve. The most notable feature of the disk structure is a thickening of the rim in the direction corresponding to phase ~0.8. The emission from the accretion disk and the inward facing side of the raised rim of the disk is assumed to be dominated by reprocessed X-rays. Emission from the outside of the disk rim and the X-ray heated face of the companion star is also important. Such a model reproduces well the observed shape of the light curve of 2A 1822–371 in all spectral regions. We also discuss qualitatively how a similar model can account for the slight asymmetries found in the optical light curves of the X-ray binaries 4U 2129+47 and HZ Her.

The model fits to the light curve of 2A 1822–371 suggest that the orbital inclination of the binary system is 76°–84°, and that its distance is between 1 and 5 kpc with a most probable distance in the range 2–3 kpc. The observed X-ray flux of the source thus corresponds to an isotropic luminosity of $\sim 10^{36}$ ergs s$^{-1}$.

*Subject headings:* stars: individual — X-rays: binaries

## I. INTRODUCTION

The X-ray source 2A 1822–371 (=V691 CrA) may be prototypical of a class of accreting close binary system in which the X-ray emission is diffused by a cloud of ionized material that is associated with the accretion disk (White and Holt 1982; hereafter WH). Other members of this class include 4U 2129+47 (=V1727 Cyg) and possibly Cyg X-3 (WH; McClintock *et al.* 1982). The 5.57 hr orbital period of 2A 1822–371 is manifest as a modulation of the system's optical light (Mason *et al.* 1980; hereafter M80), X-radiation (White *et al.* 1981), and ultraviolet emission (Mason and Córdova 1982, hereafter MC) as well as its optical emission line strength and radial velocity (Mason *et al.* 1982; Cowley, Crampton, and Hutchings 1982). The light curve of the star is complex and differs considerably in shape between the various wavelength bands in which it has been observed.

Following earlier qualitative suggestions (M80; White *et al.* 1981; MC), WH have modeled the X-ray light curve in terms of obscuration of the diffuse X-ray source by a disk rim whose height is a function of azimuthal angle, coupled with a partial occultation by the mass donating companion star. Their work suggests that there are in fact two main projections or bulges on the disk rim: one at the point where the disk is intercepted by the gas stream from the companion (see Lubow and Shu 1976) and a second, smaller bulge on the opposite side of the disk. This result is corroborated by the optical spectroscopy of Mason *et al.* (1982) which requires two regions of enhanced He II 4686 Å line emission on the disk at similar phases to the bulges inferred by WH. If this interpretation is correct, we have in 2A 1822–371 and sources like it an opportunity to study the vertical

[1] Visiting Astronomer at the Infrared Telescope Facility which is operated by the University of Hawaii under contract from the National Aeronautics and Space Administration.

[2] Work begun at Space Sciences Laboratory, University of California, Berkeley.

TABLE 1

JOURNAL OF OBSERVATIONS

| Night | Date (1981 U.T.) | Time (U.T.) | Phase | Data |
|---|---|---|---|---|
| 1 .................. | Aug 18 | 06:36–09:53 | 0.24–0.83 | *J*, *H*, *K* |
| 2 .................. | Aug 19 | 05:41–07:29 | 0.38–0.71 | *J*, *H* |
| 3 .................. | Aug 20 | 05:34–08:24 | 0.67–0.18 | *J*, *H* |
| 4 .................. | Aug 21 | 05:51–10:04 | 0.03–0.79 | *J*, occasional *H* |

structure of accretion disks in X-ray binaries in great detail.

In the present paper we report on infrared photometry of 2A 1822−371 in the *J* (1.25 μm), *H* (1.65 μm), and *K* (2.2 μm) bands. A complete 5.57 hr light curve has been obtained at *J* which allows us to extend the investigations of the energy dependence of the ultraviolet and optical curve begun in MC. We also extend the modeling of WH to the long wavelength light curve by incorporating the influence of emission from the inner and outer rim of the disk and from the companion star. Including such effects, and assuming that reprocessed X-rays are the major source of light at $\lambda > 1100$ Å, we are able to reproduce the morphology and energy dependence that is observed in the light curve of 2A 1822−371 from the far-ultraviolet to the near-infrared.

## II. INFRARED OBSERVATIONS

The infrared data were obtained on four successive nights beginning on 1981 August 17–18, using the 3.0 m NASA Infrared Telescope Facility on Mauna Kea and the Insb detector cooled with liquid helium. A chopping frequency of 10 Hz was used, and background was sampled 20″ from the target star at a position previously determined to be free from contamination by random field objects. The aperture size employed was 8″. A journal of the observations is contained in Table 1 which includes the binary phase intervals covered. Flux calibration standards were measured before and after each observation and at various zenith distances throughout the night. These data enabled us to correct for extinction and for slight variations in the efficiency of the detector from night to night.

Figure 1 shows the data taken in the *J* filter on nights 3 and 4 folded on the 5.57 hr period using the ephemeris given in Table 2. Because of the high zenith distance of 2A 1822−371 at Mauna Kea, the 5.57 hr cycle could not be observed in its entirety on any one night. The observing times on nights 3 and 4 were chosen to provide complementary phase coverage. Each data point represents a 4 minute integration, while the error bars are based on the standard deviation of 20 s samples within each 4 minute interval. Because of dead time associated with beam switching and filter changes, the start times of neighboring 4 minute integrations are separated on average by about 5 minutes. On night 3, measurements with the *J* and *H* filter were made in alternate 4 minute integrations, further reducing the sampling frequency in each filter. However on night 4, measurements in the *H* filter were made only occasionally in order to obtain the best possible time resolution in the *J* band. A nearby

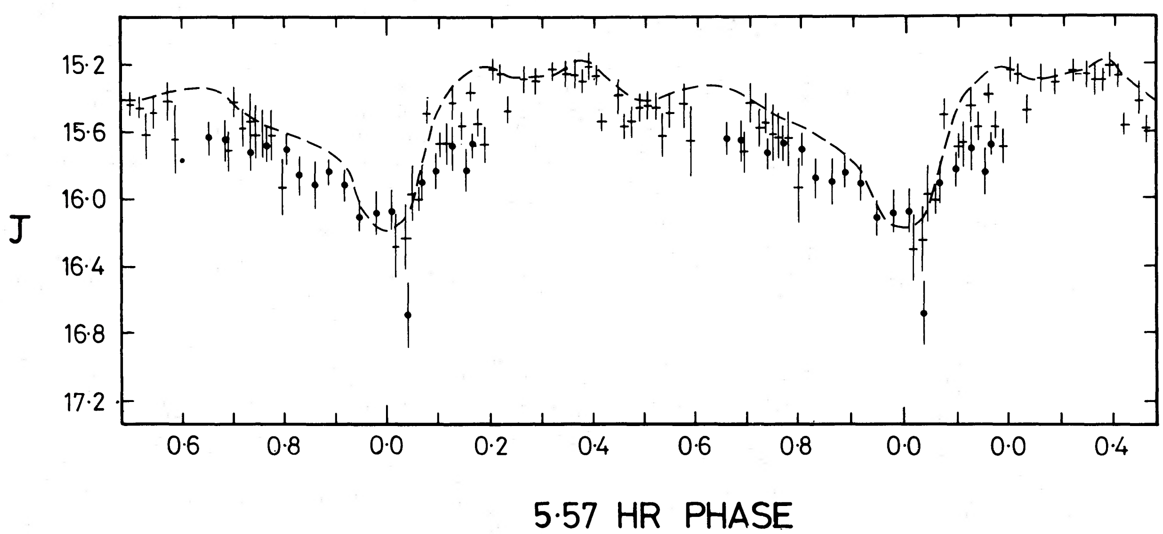


FIG. 1.—Light curve of 2A 1822−371 taken in the 1.25 μm (*J*) band. Data from night 3 (*solid circles*) and night 4 (*horizontal lines*) have been combined by folding on the 5.57 hr period of the star and together give complete phase coverage of the cycle. The *B* band light curve of M80 (*dashed line*) is shown on the same scale.

SAO star was also observed occasionally during the run on night 4 as a check of the photometric quality of the data, although conditions appeared to be photometric on all four nights. When subjected to the same reduction process as the 2A 1822−371, the count rate on the comparison star was found to be stable to within 5%.

The resulting $J$ light curve of 2A 1822−371 is remarkably similar to optical light curves of the star obtained with a similar precision and sampling rate (for example, the photographic photometry shown in Fig. 2 of M80). The curve is asymmetric, with a gradual decline, possibly steepening toward the minimum, and a more rapid rise. In order to facilitate a more detailed comparison with the optical curve, we have overlayed the photoelectric $B$ band light curve of M80 in Figure 1. The two curves are consistent within the uncertainties of the infrared points except possibly in the phase intervals 0.6–0.9 and 0.1–0.2 where the infrared curve may be slightly deficient with respect to the optical. The overall depth of the modulation is the same in the two bands. This indicates that the marked energy dependence that characterizes the ultraviolet light curve is largely absent at longer wavelengths.

Measurements in three wavebands on night 1 spanning the phase interval 0.4–0.9 yielded a mean $J$ magnitude of $15.68 \pm 0.07$ and colors $(J-H) = -0.02 \pm 0.17$, $(H-K) = 0.10 \pm 0.3$. Measurements in $H$ and $K$ on the other nights were consistent with these colors, and no dependence on orbital phase was detected. The maximum $J$ magnitude measured on night 4 between phase 0.2 and 0.4 was 15.24. Since no evidence of long term variability in the emission from 2A 1822−371 has ever been observed, we have combined the non-simultaneous ultraviolet, optical, and infrared measurements of the star at maximum light in order to study the overall spectrum. The measurements of 2A 1822−371 in the infrared are consistent with a Rayleigh-Jeans extension of the optical spectrum ($F_\lambda \alpha \lambda^{-4}$), confirming the thermal nature of the emission suggested by fits to the ultraviolet and optical data alone (MC). Both the models that were successfully fitted in MC to the data from 1100 to 5500 Å are consistent with the infrared points: a single blackbody with a temperature of $\sim 2.7 \times 10^4$ K reddened by an amount corresponding to a color excess $E_{B-V} = 0.2$, and a steady state, optically thick disk spectrum with $T_* = 1.2 \times 10^5$ K, $R_{\text{out}}/R_{\text{in}} = 30$ and $E_{B-V} = 0.1$. The latter model is probably not appropriate for 2A 1882−371 in view of our discussion of its light curve in subsequent sections, but it illustrates that multitemperature spectra can represent the data as well as an isothermal model within the allowed range of reddening. The ultraviolet, optical, and infrared spectrum of 2A 1822−371 is discussed further in § IV.

## III. THE MODEL

As noted in § I, WH have been successful in reproducing the X-ray light curve of 2A 1822−371 with a model in which a large, X-ray scattering accretion disk corona is partially occulted by the mass donating companion star and by vertical projections on the outer edge of the accretion disk. We now assess whether this model can be reconciled with the ultraviolet, optical, and infrared data. For the purposes of the numerical calculation we adopt a simplified model for the system in which a planar accretion disk is surrounded by a thin "wall" of height $h(\psi)$, where $\psi$ is the azimuth angle of the disk. Because the disk has a finite thickness at its outer edge, the inside of the wall is only visible above a height $H = 0.05\, R_d^{1.125}\, R_\odot$, which is the standard thin disk radius-height relation with $R_d$ equal to the outer radius of the disk. Following the suggestions in MC, we consider four contributions to the long wavelength modulation. These are:

1. Obscuration of the disk, and the inner face of the wall on the far side of the disk, by the section of the wall that is closest to the observer. This is similar to the way in which the broad component of the X-ray modulation is thought to arise.
2. A component that describes the projected area of the visible portion of the wall's inner face as a function of orbital phase.
3. A component that describes the projected area of the outer face of the wall as a function of orbital phase.
4. A sinusoidal component which represents the changing aspect of the X-ray heated side of the companion.

In addition, the computer code allows for a constant source of radiation such as might be contributed by the companion star, and for occultation of the various regions of the disk and wall by the companion. The size of the accretion disk and the function $h(\psi)$ which describes the vertical height of the wall as a function of azimuthal angle are determined as a function of inclination by the fits to the X-ray light curve (WH). The shape of the function $h(\psi)$ is shown in Figure 8, panel 2 of WH. We assume that the radiation from the disk and from the inner face of the wall is dominated by reprocessed X-rays [the ratio of X-ray to optical-plus-UV flux from this system is at least 5 if $E(B-V) = 0.2$]. It is also assumed initially that the emissions from these two regions have the same temperature, although the effect of relaxing this assumption is also investigated. If they emit at the same temperature, their relative contribution to the observed flux is only a function of inclination. The ratio ($\eta$) of the emissivity of the outer wall to that of the inner disk is allowed to be a free parameter and reflects the difference in the effective temperatures of these two regions. If the model is correct, this difference in temperature will be such as to yield the observed energy dependence of the light curve as suggested in MC. It should be stressed that this condition is not imposed *a priori*, and so it is a test of how meaningful the fit is. No *a priori* constraints can be imposed on the function that describes the flux from the companion. This is because the degree to which it is shielded by the disk is uncertain, so that the fraction of that star's surface exposed to X-rays is unknown. Further constraints on the system are imposed by Kepler's law, the requirement that the companion star fill its Roche

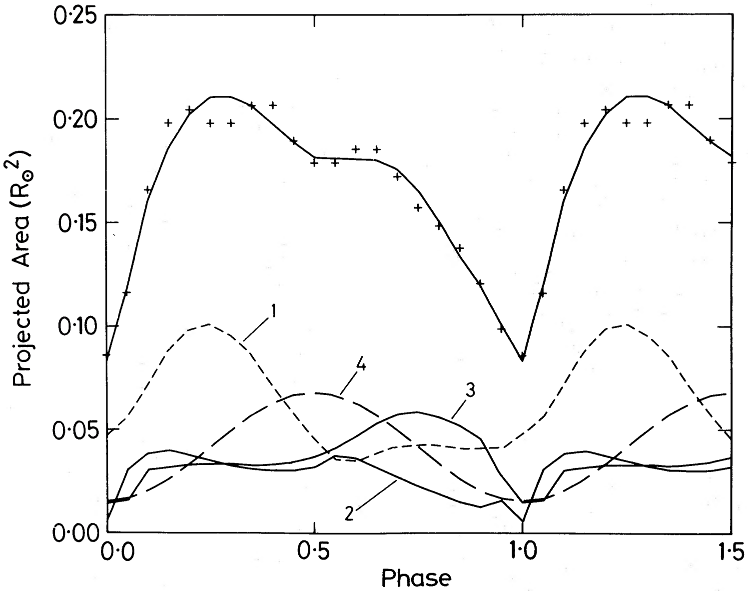


FIG. 2.—Best fit model to the $B$ band light curve of M80. The crosses are the mean $B$ band data at the appropriate phase. The four components that make up the model light curve are shown separately. They are: (1) emission from the inward facing side of the rim that surrounds the accretion disk; (2) emission from the disk; (3) emission from the outside of the rim, and (4) emission from the X-ray heated face of the companion. The ordinate is expressed in units of solar radii squared and is directly applicable to components 1 and 2 only. The emitting areas of components 3 and 4 have been scaled to fit the data as explained in the text. The projected area of component 3 is related to the value shown on the ordinate by the factor $\eta$ (see text).

lobe (the companion is in fact assumed to be spherical with a radius equal to the mean Roche radius), and measurements of the orbital velocity of the component stars.

### IV. APPLICATION TO 2A 1822−371

In the case of 2A 1822−371, the orbital velocity of the X-ray source is known (Mason *et al.* 1982; Cowley, Crampton, and Hutchings 1982), so that the binary parameters are determined for Roche geometry by the orbital inclination, the mass of the X-ray source, and the X-ray mass function. Thus, for this star, the model nominally has six free parameters: (1) a normalization constant that relates the observed and predicted flux; (2)–(4) the relative normalization of components 3, 4, and the unmodulated light; (5) the orbital inclination; and (6) the mass of the X-ray source. In practice, this is effectively reduced to five, since the shape of the light curve is only weakly dependent on the mass of the X-ray source.

To fit the model to the $B$ band optical light curve, we have determined the mean $B$ flux at 20 phase points spaced equally throughout the 5.57 hr cycle using the data in Figure 3 of M80. This sampling is sufficient to describe the gross morphology of the light curve that we seek to explain. The flux predicted by the model is computed at the same phase points and the free parameters varied according to the Marquardt algorithm (Bevington 1969) so as to minimize the variance of the model with respect to the data. Figure 2 shows the best fit model light curve computed using a value of $K_x = 70$ km s$^{-1}$ (Mason *et al.* 1982; Cowley, Crampton, and Hutchings 1982), a disk of 0.6 $R_\odot$ radius (WH), and a mass for the X-ray source of 1.4 $M_\odot$ superposed on the optical data. The agreement between the best fit model and the $B$ band data is remarkably good. The shape of the light curve, and particularly the depth of the eclipse caused by the secondary star, is very sensitive to the inclination adopted for the binary system. The best agreement between the model and the data is found for an inclination of 80°, while acceptable fits are obtained only in the range $76° < i < 84°$. If $K_x$ is increased from 70 to 100 km s$^{-1}$, which is the upper limit given by Mason *et al.* (1982), the best fit inclination is reduced from 80° to 77°. The models are not sensitive to the mass assumed for the X-ray source, $M_x$. A variation in $M_x$ from 0.8 to 2.0 solar masses causes the best fit inclination to change by only 1°. We have also tried models in which the relative normalization of the emission from the disk and the inner wall is a free parameter to allow for a possible temperature difference between these two components. The best fit is obtained with this parameter close to unity, indicating that the isothermal approximation is adequate. In addition we have examined the effects of removing the second, smaller bulge on the accretion disk (WH). Its absence can be compensated for to some extent by adjusting the normalization of the various components of the model, but the variance of the best fit is still almost twice that obtained with the second bulge present. The parameters inferred for the 2A 1822−371 system from the model fits are summarized in Table 2.

The contributions to the total light from the various modulation components as a function of phase are shown separately in Figure 2. The X-ray heated inner face of the

TABLE 2

PHYSICAL PARAMETERS OF 2A 1822−371

| Parameter | Value | Reference |
| --- | --- | --- |
| Orbital period (X-ray) | 0.232108 ± 0.000001 days | 1 |
| Epoch of X-ray minimum | HJD 2444105.674 ± 0.002 | 1 |
| $F(m)$ | 0.007 $M_\odot$ | 1 |
| Orbital inclination | 76°–84° | 2 |
| $M_x$ (assumed) | 0.8–2.0 $M_\odot$ | |
| $M_c$ | 0.20–0.35 $M_\odot$ | 3 |
| $a$ | 1.6–2.1 $R_\odot$ | 3 |
| Disk radius | 0.6 $R_\odot$ | 4 |
| Height of primary bulge (corresponding to range of inclination) | 0.21–0.11 $R_\odot$ | 4 |
| Distance | 1–5 kpc | 2 |
| $L_x$ | $1.1 \times 10^{35}$ $(d/1\ \mathrm{kpc})^2$ ergs s$^{-1}$ | 5 |

REFERENCES.—(1) Mason *et al.* 1982. (2) Present work. (3) Corresponding to assumed range of $M_x$. (4) WH. (5) White *et al.* 1981.

"wall" produces a highly modulated light curve (labeled 1 in Fig. 2) that peaks at phase ~0.25 due to the presence of the primary bulge on the accretion disk near the point where the gas stream from the companion is thought to impact the disk. This component is responsible for the sharp rise in the optical light that occurs after eclipse of the disk by the companion star. The minimum of component 1 is filled in by emission from the secondary bulge and is almost flat. At an inclination of ~80°, the total light from the heated inner face of the wall exceeds that from the disk (labeled 2 in Fig. 2) by about a factor of 2. The emission from the outer face of the wall peaks at phase ~0.75 (curve 3 in Fig. 2), while the emission from the heated face of the companion (curve 4 in Fig. 2) is a maximum at phase 0.5. Curves 3 and 4 together cause the shoulder in the light curve between phase ~0.5 and ~0.8. Component 3 is similar to the light curves of some cataclysmic variables (e.g., the dwarf nova U Gem during optical quiescence; Warner 1976) in having a pronounced "hump" prior to the eclipse by the companion star. In the cataclysmic variables the hump is often attributed to a bright spot on the disk, but in the present model the surface brightness of the outer wall is constant, and only the projected area changes.

It should be noted that the eclipse by the companion star has a different shape for each of the emission components. The eclipse of the side of the wall that is closest to the observer and the companion star is the broadest, and, because of the bulge, its centroid occurs slightly later than phase zero. The eclipse of the disk by the companion is less marked, while the far side of the wall is not eclipsed at all at an inclination of 80°.

The best fit to the $B$ band data was obtained with the emissivity of the outer face of the wall (curve 3) scaled with respect to the X-ray heated inner disk by a factor of $\eta = 0.23^{+0.02}_{-0.10}$. The emission from the outside of the wall is thus cooler than that from the inside, as might be expected. The uncertainties in $\eta$ correspond to the range of inclination angle cited above. The normalization of component 3 is not sensitive to the fraction of the flux contributed by the heated face of the companion (curve 4). In order to compare the predicted and observed energy dependence of the light curve, we estimate the effective temperatures of the X-ray heated disk and the outside wall. To do this, we have modeled the spectrum of the star at maximum light with two reddened blackbody spectra whose relative normalization is such as to yield a flux ratio in the $B$ band (4400 Å) that is consistent with the value of $\eta$ derived from the model light curve. Blackbody spectral models are adopted for ease of parameterization and because the overall spectrum at maximum light (which, according to the model, should be made up chiefly of emission from the X-ray heated disk and inner wall) is well approximated by a blackbody shape. The spectral fit is illustrated in Figure 3. We obtain an effective temperature for the X-ray heated disk of $2.85 \times 10^4$ K, an effective temperature for the outer wall of $1.45 \times 10^4$ K, and $E_{B-V} = 0.2$. We stress that we cannot distinguish this model from a single blackbody fit on the basis of the spectral data alone; the motivation for the two component spectrum comes entirely from the light curve model.

Using these effective temperatures we can compare the predicted energy dependence of the light curve with that observed. The far-UV light curve of 2A 1822−371 has a shape that resembles the X-ray light curve more than the optical light curve (MC); the depth of modulation in the far-UV, however, is about twice as great as in the X-ray band. The temperature of $1.45 \times 10^4$ K inferred for the emission from the outside wall is such that this region should contribute little to the total flux at 1400 Å (Fig. 3). If we remove this component from the model, the light curve is indeed found to be qualitatively similar to the X-ray curve, but with a higher depth of modulation. The ultraviolet light curves of MC can be used to determine the relative contribution of the outer wall to the total light as a function of wavelength, and thus obtain another,

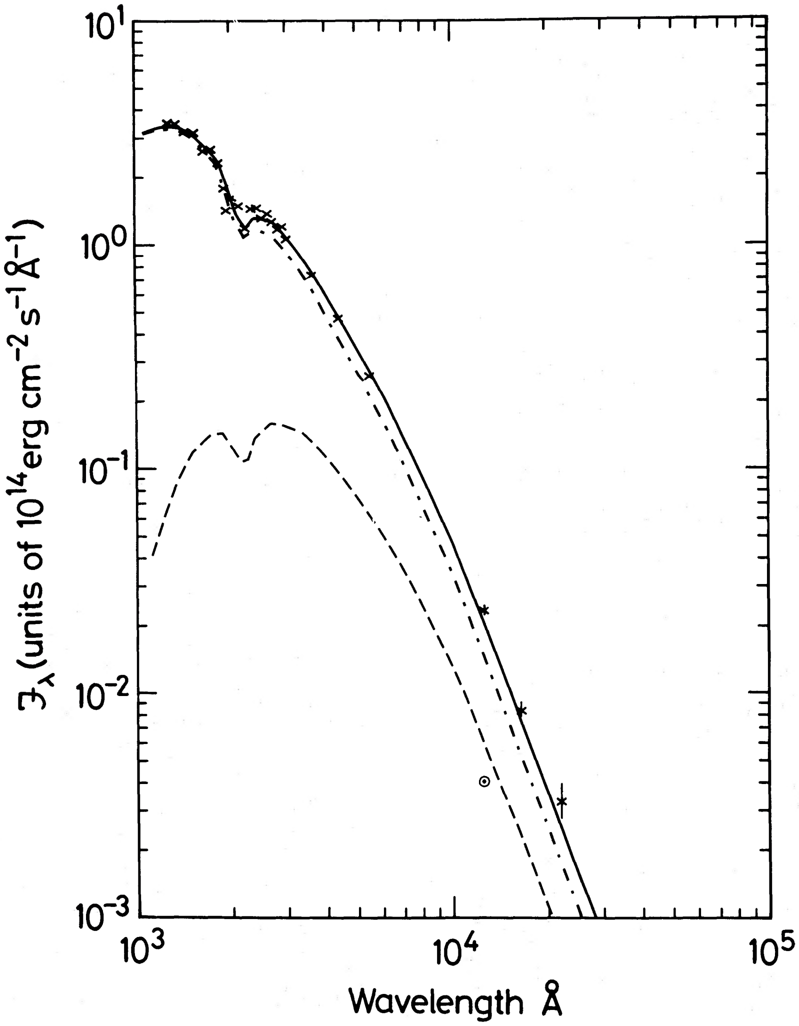


FIG. 3.—The measured spectrum of 2A 1822−371 at maximum light (*crosses*) using data from MC, M80, and the present work. The solid line is the best fit two-component blackbody model. The lower temperature component represents the emission from the outward facing part of the disk rim, and its normalization with respect to the hotter component has been constrained to agree with the model fitted to the $B$ band light curve. The dotted circle at 1.25 $\mu$m is the flux from the outer rim derived from the model for the 1.25 $\mu$m light curve.

independent estimate of the outer wall temperature. We have computed the flux expected from the model in the phase intervals covered by the *IUE* exposures of MC and varied the normalization, $\eta$, of the emission from the outer wall in order to obtain the best fit to the *IUE* data in various wavelength intervals. Good agreement is obtained between the measured value of $\eta$ as a function of wavelength and that expected for the effective blackbody temperature of $1.45 \times 10^4$ K derived from the optical light curve. This demonstrates the self-consistency of the modeling. The best fit to the shortest UV wavelength bin in MC, 1200–1600 Å, is, as expected, obtained with zero contribution from the outer wall; the predicted and observed data points in this wavelength interval are illustrated in Figure 4. Also shown, for comparison, is the model with $\eta = 0.23$ (i.e., the optical light curve) binned in the same way. The improvement in the fit obtained by reducing $\eta$ is clear.

The best fit of the model to the infrared light curve is shown in Figure 5. The model parameters derived are very similar to those for the optical light curve, except that the outer wall contributes proportionally $\sim 10\%$ less in the infrared; this corresponds to the relative deficiency in the infrared count rate between phase 0.6 and 0.2 noted in § II. The $J$ band flux of the outer wall that is deduced from the model light curve at maximum light is plotted in Figure 3. This flux lies about 30% below the extrapolation of the $1.45 \times 10^4$ K blackbody spectrum derived from the optical and UV data. In fact, the dereddened $B-J$ color of the outer wall ($\sim -0.5$) is closer to that expected for a stellar atmosphere with the same effective temperature and log $g = 4$ ($B-J = -0.4$; Kurucz 1979) than to the blackbody ($B-J = -0.07$). It is not surprising that the spectrum of the outer wall departs from the blackbody spectrum in this way, since the radiation it emits is

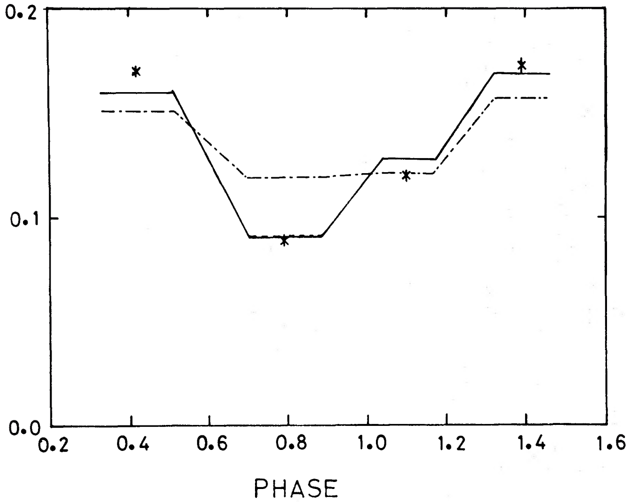


FIG. 4.—Four-point *IUE* light curve of 2A 1822−371 in the 1230–1600 Å band (*stars*) taken from MC. The dash-dot curve is the optical light curve binned in the same way; the solid curve is the distribution obtained when component 3 is removed.

presumably diffused through the "wall" from the hot inner disk. However, the Kurucz model predicts a value of $\eta = 0.08$ in the 1200–1600 Å band which is only marginally consistent with the measured far-UV light curve. It is thus probable that neither of these models exactly represents the spectrum of the outer wall over the entire wavelength range from 1200 Å to 12500 Å. It should in principle be possible to investigate the

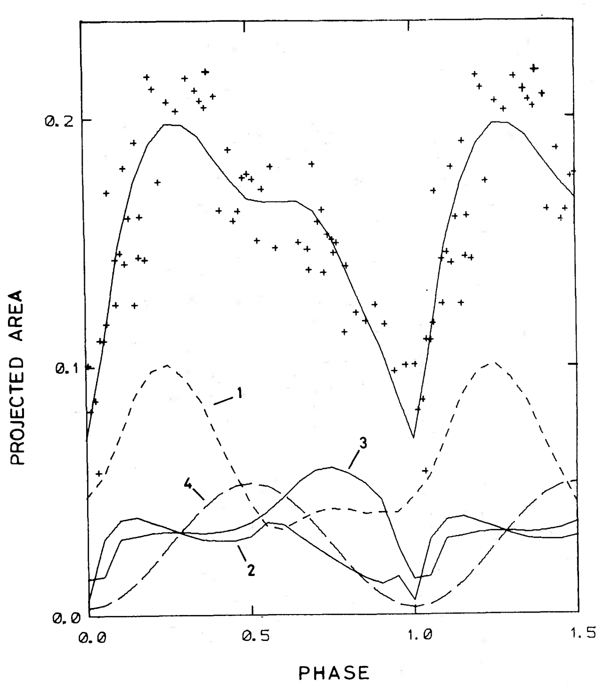


FIG. 5.—Similar fit to that described for Fig. 2 but for the *J* band data from nights 3 and 4 (*crosses*) shown in Fig. 1.

spectrum of this emission in more detail when higher time resolution UV light curves become available.

## V. THE OPTICAL EMISSION LINES

The strength of the H II 4686 Å emission line in the optical spectrum of 2A 1822−371 is modulated by about a factor of 2 with the 5.57 hr cycle (Mason *et al.* 1982). The emission line peaks at about phase 0.75 and is at minimum intensity at about phase 0.25. This is similar to the behavior of component 3 in the model light curve (the emission from the outer wall) and supports the previously suggested association of the emission lines with the outer rim of the disk (Mason *et al.* 1982). There is no evidence for an eclipse of the emission line region by the companion star in the data of Mason *et al.* (1982), but the scatter in the data is comparatively large and the expected eclipse of component 3 is partial ($\sim 50\%$). The profile of the He II line can be represented as broad base, upon which is superposed two narrower components whose velocities vary in a manner that suggests that they are associated with the primary and secondary bulges, respectively, on the disk. The extreme range of velocity variation in the peak of the He II line is $\sim 650$ km s$^{-1}$, while the width of the line at its base is about 900 km s$^{-1}$. This is somewhat lower than expected if the line producing region is orbiting at the velocity of material in the outer part of the disk. The orbital velocity should be $\sim 600$ km s$^{-1}$ (i.e., full width 1200 km s$^{-1}$) if the mass of the X-ray source is $\sim 1.4\ M_\odot$ and the radius of the disk is $\sim 0.6\ R_\odot$. The low observed velocity could be explained if the line emitting region were lower velocity material orbiting at larger distances from the X-ray source than the outer "edge" of the disk, or if projection effects were important in determining the line profile.

## VI. THE DISTANCE AND LUMINOSITY OF 2A 1822−371

The model fits to the light curve of 2A 1822−371 yield measurements of the emitting area of various components of the system which can be used to estimate the distance of the star. At phase $\sim 0.25$ (maximum light) the projected area of the outer wall is $0.15^{+0.03}_{-0.02}\ R_\odot^2$, where the uncertainties correspond to the allowed range of orbital inclination of the system. If it is assumed that the outer wall has the same surface brightness as a star with the same effective temperature (spectral class mid-B), we obtain a distance for the system of $2.0 \pm 0.9$ kpc. The uncertainty in the distance includes the uncertainty in the projected area of the wall and also the effects of varying the degree of reddening from $E_{B-V} = 0.1$ to $E_{B-V} = 0.3$. Alternatively, the projected area of the inner wall at maximum light is $0.10^{+0.03}_{-0.05}\ R_\odot^2$. If we assume that the inner wall radiates as a blackbody with a temperature in the range $2.5\text{–}3.0 \times 10^4$ K (corresponding to spectral fits with $0.1 < E_{B-V} < 0.3$), we obtain a distance of $3.1 \pm 1.5$ kpc for 2A 1822−371. The blackbody approximation represents the maximum emissivity of the wall, so the latter estimate is an upper limit to the distance of the source.

The X-ray luminosity required to heat the inside of the wall to the observed temperature, $T$, is $4\pi R_d^2 \sigma T^4$, where $R_d$ is the radius of the disk. Adopting $R_d = 0.6\ R_\odot$ (WH) we obtain $L_x$(predicted) $= 7 \pm 3 \times 10^{35}$ ergs $s^{-1}$. The measured 2–60 keV X-ray flux of 2A 1822−371 is $1 \times 10^{-9}$ ergs $cm^{-2}$ $s^{-1}$ (White *et al.* 1981) which implies an X-ray luminosity of $1.1 \times 10^{35}$ $(d/1\ \mathrm{kpc})^2$ ergs $s^{-1}$. Agreement between the predicted and observed luminosities is obtained for $1.9 < d < 3.0$ kpc, consistent with the previous distance estimates.

## VII. 4U 2129+47

An X-ray source that may be related to 2A 1822−371 is 4U 2129+47. It has an orbital period of 5.2 hr, and, like 2A 1822−371, it exhibits a gradual and partial X-ray eclipse that betrays the presence of a diffusing cloud around the X-ray source (WH; McClintock *et al.* 1982; Ulmer *et al.* 1980). Some of the X-ray measurements of 4U 2129+47 also show a broad minimum prior to the eclipse that could be symptomatic of structure on the outer accretion disk similar to that seen in 2A 1822−371. However, the feature may be transient (WH), and no attempt has been made to model the accretion disk structure of 4U 2129+47 because of the relatively poor statistical precision of the X-ray data.

The optical light curve of 4U 2129+47 is quasi-sinusoidal (Thorstensen *et al.* 1979; McClintock, Remillard, and Margon 1981) and is thus quite different from that of 2A 1822−371. The similarity to the optical light curve of the X-ray binary HZ Her/Her X-1 has been noted, and both curves are interpreted as being due to the changing visibility of the X-ray heated face of the mass donating star as it orbits its compact companion. The light curves of both HZ Her and 4U 2129+47, however, show small but significant departures from a perfect sinusoid. In both cases, the minimum is narrower than the maximum, while the ascending part of the light curve is slightly steeper than the decline.

McClintock *et al.* (1982) and WH have suggested that the orbital plane of 4U 2129+47 is more highly inclined to the line of sight than 2A 1822−371, so that the inner, luminous parts of the disk are hidden and the heated face of the companion is more prominent. To investigate the feasibility of this suggestion, we have examined the effects of increasing the orbital inclination in our model. Because we do not know the parameters that describe the structure of the accretion disk in 4U 2129+47, we have not attempted to formally fit the optical light curve of the star. Instead we adopt, for illustration, the best fit parameters for 2A 1822−371. Figure 6 (*left*) shows such a model computed at an inclination of 89°. Also plotted for comparison is the *B* band light curve of 4U 2129+47. The latter points were computed at the appropriate phase values from the parameters given by McClintock, Remillard, and Margon (1981) for a fit of an abridged Fourier series to their light curve VI, except that the point at zero phase has been reduced by 20% to correspond more exactly to their observed data. At this inclination the disk (component 2) is not visible at all in the model, while the inner wall (component 1) is almost entirely obscured between phase 0.5 and 0.0. The fraction of the total light contributed by the companion is, as expected, increased compared to that at the inclination of 2A 1822−371, but the shape of the resulting light curve, which is made up of emission from the outer wall, the inner wall and the companion, is not a good match to the observed light curve of 4U 2129+47. A much better correspondence is obtained if the relative contribution from the companion is increased by about a factor of 8 as shown in Figure 6 (*right*). The resulting light curve is slightly asymmetrical in the same sense as the observed data because of the contributions from

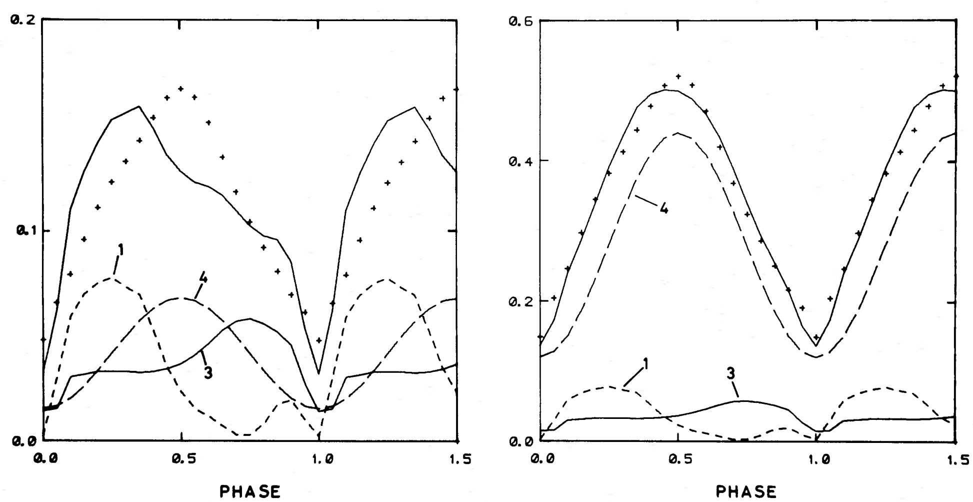


FIG. 6.—The crosses are the *B* band light curve of 4U 2129+47 given by McClintock, Remillard and Margon 1981 (their curve VI). The left-hand panel compares these data with the best fit model derived for 2A 1822−371 seen at an inclination of 89°. The model shown in the right-hand panel has the same parameters except that the contribution from component 4 has been increased by about a factor of 8.

components 1 and 3, while the minimum is narrower than the maximum because of the eclipse of the disk emission by the companion. It appears, therefore, that the optical light curve of 4U 2129+47 (and perhaps also HZ Her) could be modeled in the same way as that of 2A 1822−371 if the emission from the companion were increased or alternatively if the disk components were relatively less luminous. It will be interesting to fit detailed models to the data on 4U 2129+47 when higher quality X-ray light curves become available.

## VIII. DISCUSSION

We have shown that the light curves of 2A 1822−371 in the ultraviolet, optical, and infrared bands can be accurately reproduced using the same accretion disk structure deduced by WH to explain the X-ray light curve, provided that X-ray heating of the disk and the companion star and the intrinsic emission of the outer rim of the disk are included in the model. A temperature difference between the parts of the disk subjected to direct X-ray heating and the outer edge of the disk naturally explains the energy dependence of the light curve which is most apparent in the ultraviolet range. The ability of this comparatively simple model to reproduce the apparent morphological complexity and energy dependence of the light curve of 2A 1822−371 from X-ray to infrared wavelengths provides confidence that it is correct. Its most important feature is a bulge on the outer edge of the disk at a phase generally associated with the point of impact of the mass transfer gas stream from the companion. The thickness of the bulge in 2A 1822−371 is about 3 times the thickness of the outer edge of the disk.

The conditions of orbital inclination and X-ray luminosity in 2A 1822−371 are such as to show the effects of the bulge to good advantage. Similar accretion disk structure may also, however, be present in other interacting binary sources. In § VII we showed how the model for 2A 1822−371 could account qualitatively for the properties of the optical light curves of 4U 2129+47 and HZ Her if the ratio of the emission from the disk to that from the companion is much less than in 2A 1822−371. Walter *et al.* (1982) and White and Swank (1982) have observed periodic dips in the X-ray flux of the X-ray burst candidate 4U 1916−05 which can be interpreted as obscuration of the central X-ray source by vertical projections on the disk surrounding it. A number of authors have also inferred the existence of azimuthal structure in the thickness of the accretion disks around cataclysmic variables that is similar to that required for 2A 1822−371 (e.g., Hassall *et al.* 1981; Chester 1979; Alpar 1979). In addition, the well-known hump in the light curve of a few cataclysmic variables, which has usually been interpreted as a bright spot on the accretion disk, may also be explainable as a thickening of the outer disk with no increase in surface brightness. Thus, information derived on the structure of the accretion disk in 2A 1822−371 may well be applicable to a large number of sources.

Another interesting property of 2A 1822−371 is the scattering cloud that diffuses the X-ray source. WH measure the effective size of the cloud to be $\sim 2 \times 10^{10}$ cm and note that the optical depth to the X-ray source must be about 5 in order to account for the breadth of the 6.7 keV iron line and the cutoff observed in the X-ray spectrum above $\sim 20$ keV. The cloud may be evaporated from the disk or may be generated by turbulence within the disk (see references in WH). We note that evidence has recently been found for high-velocity winds from the disks of a number of cataclysmic variable systems (e.g., Córdova and Mason 1982), suggesting that there may be a substantial envelope of low density material surrounding the disk in many of these accreting systems. Fabian, Guilbert, and Ross (1982) have simulated the observed X-ray spectrum of 2A 1822−371 by radiative transfer through a shell of gas and determine that most of the scattering cloud must lie within $10^8$ $(L_x/10^{37}$ ergs s$^{-1})$ cm from the source. In order to account for the measured radius of the cloud of $2 \times 10^{10}$ cm, it is necessary to postulate that much of this volume is occupied by optically thin gas (see also McClintock *et al.* 1982 and MC). The observed X-ray flux of 2A 1822−371 corresponds to an isotropic luminosity, $L_x$, of about $10^{36}$ ergs s$^{-1}$ at a distance of about 2.5 kpc. However, this probably underestimates the true luminosity of the source because scattered photons will tend to escape preferentially in directions perpendicular to the disk plane if, as is likely, the density of gas above the disk falls off with increasing height.

The evidence suggests that 2A 1822−371 might be a typical member of the bulge population of X-ray sources, but seen at high inclination. Its rather low X-ray luminosity and low ratio of X-ray to optical flux could be a consequence of the scattering cloud and a high orbital inclination as discussed above. Recent optical photometry of two other galactic bulge sources, XB 1636−53 and XB 1735−44, suggests that they may have orbital periods of about 4 hr (see van Paradijs, Pedersen, and Lewin 1981 and McClintock and Petro 1981) similar to those of 2A 1822−371 and 4U 2129+47. It has also been noted by Fabian, Guilbert, and Ross (1982) and others that a hot Comptonizing cloud similar to that required in 2A 1822−371 has been postulated to explain the X-ray spectra and spectral variability that is observed in many of the bright bulge sources (Branduardi *et al.* 1980; Lamb and Sanford 1979; Mason *et al.* 1976).

We are grateful for the hospitality and assistance of the IRTF staff and are particularly grateful for the advice and assistance of Dr. Eric Becklin, Dr. Ian Gatley, and the telescope operator Ron Koehler. This work was supported by the US Department of Energy (F. A. C.), NASA grant NAGW-44 (K. O. M.), and the U.K. Science and Engineering Research Council (K. O. M.).

## REFERENCES


Alpar, M. A. 1979, *M.N.R.A.S.*, **189**, 305.
Bevington, P. R. 1969, *Data Reduction and Error Analysis for the Physical Sciences* (New York: McGraw-Hill).
Branduardi, G., Kylafis, N. D., Lamb, D. Q., and Mason, K. O. 1980, *Ap. J.* (*Letters*), **235**, L153.
Chester, T. J. 1979, *Ap. J.*, **230**, 107.
Córdova, F. A., and Mason, K. O. 1982, *Ap. J.*, **260**, 716.
Cowley, A. P., Crampton, D., and Hutchings, J. B. 1982, *Ap. J.*, **255**, 596.
Fabian, A. C., Guilbert, P. W., and Ross, R. R. 1982, *M.N.R.A.S.*, in press.
Hassall, B. J. M., Pringle, J. E., Ward, M. J., Whelan, J. A. J., Mayo, S. K., Echevarria, J., Jones, D. H. P., and Wallis, R. E. 1981, *M.N.R.A.S.*, **197**, 275.
Kurucz, R. L. 1979, *Ap. J. Suppl.*, **40**, 1.
Lamb, P. L., and Sanford, P. W. 1979, *M.N.R.A.S.*, **188**, 555.
Lubow, S. M., and Shu, F. M. 1976, *Ap. J.* (*Letters*), **207**, L53.
Mason, K. O., and Córdova, F. A. 1982, *Ap. J.*, **255**, 603 (MC).
Mason, K. O., Charles, P. A., White, N. E., Culhane, J. L., Sanford, P. W., and Strong, K. T., 1976, *M.N.R.A.S.*, **177**, 513.
Mason, K. O., Middleditch, J., Nelson, J. E., White, N. E., Seitzer, P., Tuohy, I. R., and Hunt, L. K. 1980, *Ap. J.* (*Letters*), **242**, L109 (M80).
Mason, K. O., Murdin, P. G., Tuohy, I. R., Seitzer, P., and Branduardi-Raymont, G. 1982, *M.N.R.A.S.*, in press.
McClintock, J. E., London, R. A., Bond, H. E., and Grauer, A. D. 1982, *Ap. J.*, **258**, 245.
McClintock, J. E., and Petro, L. D. 1981, *IAU Circ.* 3615.
McClintock, J. E., Remillard, R. A., and Margon, B., 1981, *Ap. J.*, **243**, 900.
Thorstensen, J., Charles, P. A., Bowyer, S., Briel, U. G., Doxsey, R. E., Griffiths, R. E., and Schwartz, D. A. 1979, *Ap. J.* (*Letters*), **233**, L57.
Ulmer, M. P., *et al.* 1980, *Ap. J.* (*Letters*), **235**, L159.
van Paradijs, J., Pedersen, H., and Lewin, W. H. G. 1981, *IAU Circ.* 3628.
Walter, F. M., Bowyer, S., Mason, K. O., Clark, J., Henry, P., Halpern, J., and Grindlay, J. 1982, *Ap. J.* (*Letters*), **253**, L67.
Warner, B. 1976, in *IAU Symposium 73*, *The Structure and Evolution of Close Binary Systems*, ed. P. Eggleton, S. Mitton, and J. Whelan (Dordrecht: Reidel), p. 85.
White, N. E., Becker, R. H., Boldt, E. A., Holt, S. S., Serlemitsos, P. J., and Swank, J. H. 1981, *Ap. J.*, **247**, 994.
White, N. E., and Holt, S. S. 1982, *Ap. J.*, **257**, 318 (WH).
White, N. E., and Swank, J. 1982, *Ap. J.* (*Letters*), **253**, L61.


F. A. Córdova: MS D436, Los Alamos National Laboratory, Los Alamos, NM 87545

K. O. Mason: Mullard Space Science Laboratory, Holmbury St. Mary, Nr. Dorking, Surrey, RH5 6NT, United Kingdom